

Ultracold three-body collisions near narrow Feshbach resonances

Yujun Wang,¹ J. P. D’Incao,² and B.D. Esry¹

¹*Department of Physics, Kansas State University, Manhattan, Kansas, 66506, USA*
²*JILA, University of Colorado and NIST, Boulder, Colorado, 80309-0440, USA*

We study ultracold three-body collisions of bosons and fermions when the interatomic interaction is tuned near a narrow Feshbach resonance. We show that the width of the resonance has a substantial impact on the collisional properties of ultracold gases in the strongly interacting regime. We obtain numerical and analytical results that allow us to identify universal features related to the resonance width. For narrow resonances, we have found a suppression of all inelastic processes in boson systems leading to deeply bound states and an enhancement for fermion systems.

PACS numbers:

Strongly interacting three-body systems play an important role in a great many areas of physics including condensed matter, atomic, molecular and nuclear physics [1, 2]. With the recent advances in the control of interatomic interactions, ultracold atomic gases have rapidly become a preferred test bed for many interesting physical phenomena. One of the most important tools for this control is the Feshbach resonance [3]. Applying a magnetic field, the *s*-wave two-body scattering length a between two atoms can be tuned from $-\infty$ to $+\infty$, allowing for the study of systems from non-interacting to strongly interacting. A major experimental difficulty encountered in the strongly interacting limit, $|a| \gg r_0$ where r_0 is the characteristic range of the interatomic interactions, is that the system becomes unstable due to three-body collisional loss of atoms and molecules.

Ultracold three-body collisions in the limit $|a| \gg r_0$ are intimately connected to a fundamental and counter-intuitive effect first predicted by the nuclear physicist Vitaly Efimov in the early 1970’s [4]. He showed that three-boson systems with $|a| \rightarrow \infty$ possess an infinite number of weakly bound three-body states even when there are no two-body bound states. These Efimov states have a profound effect on low-energy scattering observables as they lead to interference and resonance effects [6, 7] that produce distinctive features in scattering observables whenever a is increased by the factor $e^{\pi/s_0} \approx 22.7$ [4, 5].

The main processes destabilizing ultracold atomic and molecular gases are three-body recombination, $B+B+B \rightarrow B_2^*+B$ for bosons B , and vibrational relaxation, $B_2^*+B \rightarrow B_2+B$. It is well established that the three-body recombination rate K_3 for bosons displays a series of interference ($a > 0$) and resonance ($a < 0$) features as a function of a (for $|a| \gg r_0$) reflecting Efimov physics [2, 6, 7]. Explicitly [2, 32],

$$K_3^{(a>0)} = 67.1 e^{-2\eta} \left(\sin^2[s_0 \ln \frac{a}{r_0} + \Phi] + \sinh^2 \eta \right) \frac{a^4}{m}, \quad (1)$$

$$K_3^{(a<0)} = \frac{4590 \sinh(2\eta)}{\sin^2[s_0 \ln(|a|/r_0) + \Phi + 1.53] + \sinh^2 \eta} \frac{a^4}{m}, \quad (2)$$

where $s_0 \approx 1.00624$ is a universal constant and m is the

atomic mass. Atomic units are used here and throughout this Letter. While their overall behavior is determined by a , any comparison with a physical system also requires the short-range three-body parameters Φ and η which cannot, in general, be predicted from two-body physics alone [32]. Similar universality is also manifested by the $a > 0$ vibrational relaxation rate V_{rel} for bosons [2],

$$V_{\text{rel}}^{(B)} = \frac{20.1 \sinh(2\eta)}{\sin^2[s_0 \ln(a/r_0) + \Phi - 1.67] + \sinh^2 \eta} \frac{a}{m}, \quad (3)$$

and for $FF'^*+F \rightarrow FF'+F$ collisions [20, 21]

$$V_{\text{rel}}^{(F)} = C a^{-3.332}, \quad a > 0, \quad (4)$$

where F and F' are fermions in different spin states and C depends on short-range physics.

The observation of Efimov physics in ultracold gases has recently become a very active area [8, 9, 10, 11, 12, 13], yet the universal behavior of three-body systems near a narrow Feshbach resonance remains to be fully understood. While specific systems have been modeled near a resonance [16, 17, 18, 19], no simple analytical expressions like Eqs. (1)–(4) for the collision rates have yet appeared. Instead, the vast majority of our knowledge of three-body collisions, including all of the universal analytic expressions [2], uses *only* the fact that a Feshbach resonance changes a and ignores all other aspects of the resonance. It is generally assumed that this approximation works well near broad resonances and less so near narrow ones [14]. This expectation is based on the low-energy expansion of the two-body *s*-wave scattering phase shift δ ,

$$k \cot \delta = -a^{-1} + r_{\text{eff}} k^2 / 2 + \dots \quad (5)$$

where k is the wavenumber and r_{eff} is the effective range. Since $|r_{\text{eff}}|$ is inversely proportional to the resonance width [14], the second term is negligible for broad resonances, but has significant consequences for narrow resonances — even at ultracold collision energies. To be a narrow resonance in this language requires $|r_{\text{eff}}| \gg r_0$, and r_0 is on the order of 50–100 a.u. for most alkali species. A

typical narrow resonance for Rb with a width of 1 G corresponds to $r_{\text{eff}} \approx -200$ a.u. while a quite narrow one, with a width of 0.1 G, has $r_{\text{eff}} \approx -2000$ a.u [14]. We should thus expect substantial deviations from the zero-range, $r_0 \rightarrow 0$, results in Refs. [14, 23].

With this Letter, we aim to expand our knowledge of universality near a narrow Feshbach resonance. In particular, we study the dependence of ultracold three-body collision rates on r_{eff} both numerically and analytically, obtaining analytic expressions for K_3 and V_{rel} similar to Eqs. (2) and (3), verified by essentially exact numerical solutions. For identical bosons, we show that in contrast to [14], short-range three-body physics is important — even in the limit of a zero-range two-body potential. We also find a $|r_{\text{eff}}|^{-1}$ suppression of inelastic losses for all three-boson processes leading to deeply bound two-body states. For systems involving two distinguishable fermions, however, we have found that large r_{eff} has the opposite effect: it enhances the loss rates and alters their universal behavior. Both the suppression and the enhancement can be traced to the same modification of the effective three-body interaction first identified in [14].

Previous studies have addressed some aspects of these processes near a narrow Feshbach resonance and their dependence on r_{eff} . In an especially relevant work, Petrov Ref. [14] calculated the recombination rate for identical bosons with $a > 0$ using a zero-range potential modified to include r_{eff} . By solving his model numerically, he found that the minima described by Eq. (1) still hold for $a \gg |r_{\text{eff}}|$ but occur at fixed values of $|r_{\text{eff}}|/a$ without any reference to a three-body parameter like Φ . Gogolin *et al.* [23] reproduced these results with a very different method but effectively the same physical model. Mathematically, it is true that no three-body parameter is needed since the inclusion of r_{eff} in the zero-range model regularizes it [24], removing the Thomas collapse [25]. Physically, however, we will show that a three-body parameter is still generally needed to represent the short-range three-body physics of any realistic system and that r_{eff} alone is insufficient.

To study the influence of the resonance width on the above collision rates, we numerically solved the three-body Schrödinger equation using the adiabatic hyperspherical representation [7, 33]. In this representation, the Schrödinger equation is reduced to coupled equations for the hyperradial channel functions $F_\nu(R)$,

$$\left[-\frac{1}{2\mu} \frac{d^2}{dR^2} + W_{\nu\nu} \right] F_\nu + \sum_{\nu' \neq \nu} W_{\nu\nu'} F_{\nu'} = E F_\nu, \quad (6)$$

describing both bound and scattering properties of the system. The hyperradius R represents the overall size of the system, $\mu = m/\sqrt{3}$ is the three-body reduced mass, $W_{\nu\nu}(R)$ are the effective three-body potentials obtained by diagonalizing the adiabatic (fixed R) Hamiltonian, and $W_{\nu\nu'}(R)$ are the non-adiabatic couplings governing

transitions between channels.

Although a Feshbach resonance is a multichannel phenomenon, we model it with a single-channel two-body interaction, since the asymptotic two-body scattering wave functions can be made identical for only one open channel. In other words, the asymptotic wave function does not depend on how the resonance is generated [14, 15]. The three bodies thus interact through a pair-wise sum of two-body model potentials with a barrier such as

$$v(r) = -D \text{sech}^2(3r/r_0) + Be^{-2(3r/r_0-2)^2} \quad (7)$$

which has an s -wave shape resonance. In (7), the potential depth D primarily controls a , and the barrier height B is adjusted to produce the desired r_{eff} .

Figure 1 shows our numerical calculations for K_3 and V_{rel} . We generated each curve by varying a at fixed $|r_{\text{eff}}|$, corresponding to experiments tuning across a Feshbach resonance with a particular width. For $|a| \gg |r_{\text{eff}}|$, the rates retain the features predicted in Eqs. (1)–(3) as expected. For $|a| < |r_{\text{eff}}|$, the rates deviate from these formulas, with K_3 for $a > 0$ in Fig. 1(a) approaching the $(a^7|r_{\text{eff}}|)^{1/2}$ behavior predicted in [14]. The figure also shows that the rates seem to converge to a universal curve as $|r_{\text{eff}}|$ increases once scaled properly. Moreover, the position of the first Efimov feature that appears as $|a|/|r_{\text{eff}}|$ increases agrees reasonably well with the zero-range model predictions from Refs. [14] and [23]. Note that the $K_3 a > 0$ prediction is taken directly from [14], while we have determined the $K_3 a < 0$ prediction based on the location of the first Efimov state in [23] and the V_{rel} prediction based on the position of the first pole in the atom-dimer scattering length given by [14]. Recalling that r_{eff} is only about -200 a.u. for a 1 G wide resonance, though, we see that typical experiments will actually fall far from the zero-range results. To minimize non-universal impacts of the two-body potential barrier, we have introduced a short-range hard wall in the $W_{\nu\nu}(R)$, making the short-range three-body physics more uniform as a function of r_{eff} . We have verified that the results presented in Fig. 1 are not sensitive to the precise location of this hard wall.

One of the advantages of the adiabatic hyperspherical representation is that the effective potentials offer a reasonably simple picture of the scattering processes [6, 7, 21]. Figure 2 shows a sketch of the effective three-body potentials for three identical bosons with $a \gg |r_{\text{eff}}|$ distilled from and verified by numerical solutions of the adiabatic equation for many different combinations of r_{eff} , a , and $v(r)$. The main effect of this new length scale, r_{eff} , is that $W_{\nu\nu}(R)$ for the weakly-bound molecular channel is modified in the range $r_0 \ll R \ll |r_{\text{eff}}|$, taking the Coulomb-like form $c_0/(2\mu|r_{\text{eff}}|R)$ [14] instead of the usual attractive R^{-2} Efimov potential. Our numerical analysis indicates, however, that the coefficient c_0 is not universal — even changing from attractive to repulsive

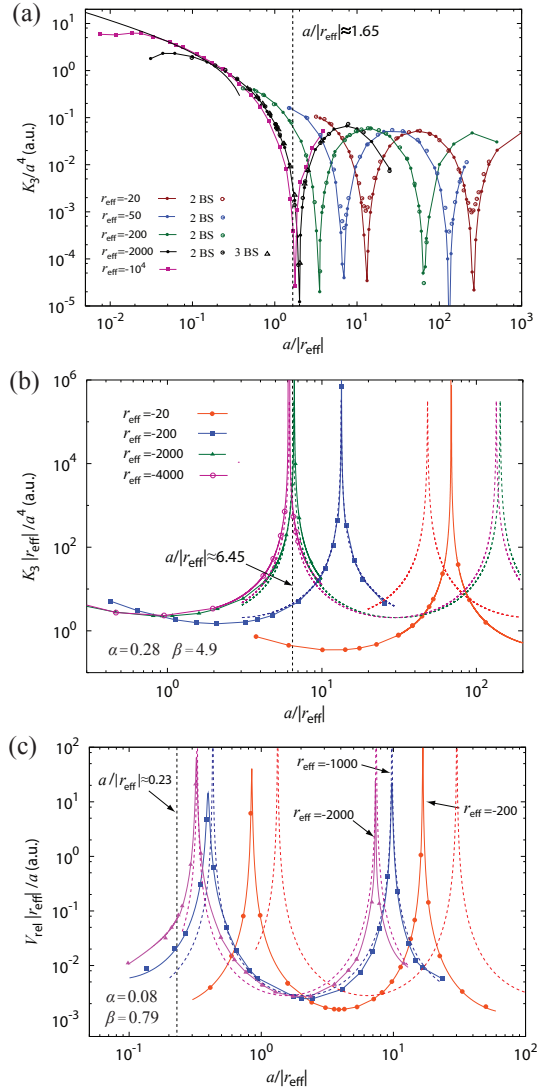


FIG. 1: Inelastic zero-energy three-body collision rates for identical bosons. The vertical dashed lines indicate the predicted position of the first Efimov feature (see [14, 23] and text). (a) Recombination rates for $a > 0$ with one or more two-body s -wave bound states as indicated. The thick solid line is the analytical result from [14] scaled to match our data. (b) Recombination rates for $a < 0$. (c) Relaxation rates for $a > 0$. The solid lines in (b) and (c) are simply to guide the eye, while the dashed lines are the analytical results from Eqs. (9) and (8), respectively, using the α and β indicated. These were fit in the limit $|r_{\text{eff}}| \rightarrow \infty$.

when a second two-body s -wave state is added and becoming increasingly repulsive as more states are added. This non-universality makes it even more surprising that the rates in Fig. 1 are universal, which we have verified by repeating the calculations with other model potentials [31] and with varying numbers of deeply bound two-body states (also shown in the figure).

The simple picture represented by Fig. 2 can also be used to derive quantitative, analytic expressions for the

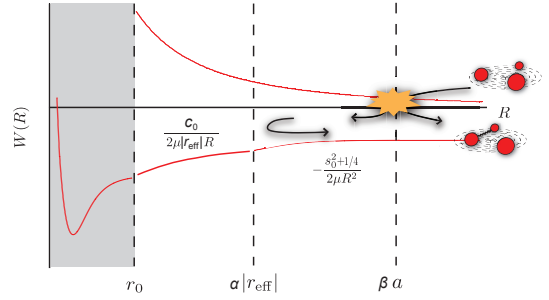


FIG. 2: The schematic three-body potentials and recombination pathways with $r_0 \ll |r_{\text{eff}}| \ll a$ for $a > 0$.

collision rates. For the case $a > 0$ shown in the figure, for instance, we calculate V_{rel} by considering incidence in the weakly bound atom-dimer channel (the lower potential in the figure) with the transition to the deeper two-body channels driven by non-adiabatic coupling localized in the region $R \leq r_0$. The hyperradial scattering wave function is found by matching the analytic solutions from each region at the boundaries $\alpha|r_{\text{eff}}|$ and $\beta|a|$, where α and β reflect the uncertainty in defining these boundaries and will be determined by fitting our final expression to the numerical results. We parametrize the solution in the short-range, non-universal, region $0 \leq R \leq r_0$ with a complex scattering length A whose imaginary part accounts for inelastic transitions. In the other non-universal Coulomb-like region, $r_0 \leq R \leq \alpha|r_{\text{eff}}|$, we take the potential to be zero since c_0 can be positive or negative without affecting the numerical results. The relaxation rate is then obtained from $V_{\text{rel}}^{(B)} = \pi(1 - \mathcal{R})/\mu k$ where \mathcal{R} is the elastic scattering probability obtained from the scattering wave function described above. The result is

$$V_{\text{rel}}^{(B)} = \frac{2\sqrt{3}\pi\beta \sin 2\varphi_0 \sinh 2\eta}{\sin^2[s_0 \ln(|a/r_{\text{eff}}|) + \Phi + \varphi] + \sinh^2 \eta} \frac{a}{m} \quad (8)$$

where $\sinh \eta = |\text{Im} A/r_{\text{eff}}| \csc(2\varphi_0) \sin^2(\Phi + \varphi_0)$ with $\varphi = s_0 \ln(\beta/\alpha) + \varphi_0$, $\tan \varphi_0 = 2s_0$, and $\tan \Phi = 2s_0(\alpha - \text{Re} A/|r_{\text{eff}}|)/(\alpha + \text{Re} A/|r_{\text{eff}}|)$. With a virtually identical analysis, $K_3^{(a < 0)}$ can be derived to be

$$K_3^{(a < 0)} = \frac{12\sqrt{3}\pi^3\beta^4 \sin 2\varphi_0 \sinh 2\eta}{\sin^2[s_0 \ln(|a/r_{\text{eff}}|) + \Phi + \varphi] + \sinh^2 \eta} \frac{a^4}{m}. \quad (9)$$

Note that α and β can take on different values than for $V_{\text{rel}}^{(B)}$ and that here $\tan \varphi_0 = s_0/2$. Similar expressions can be derived for other low-energy scattering observables.

Comparison of Eqs. (8) and (9) with Eqs. (3) and (1), respectively, shows that the expectation that r_0 is replaced by $|r_{\text{eff}}|$ is indeed true but that there are also other modifications due to $|r_{\text{eff}}|$. These expressions show, for instance, why scaling the rates in Figs. 1(b) and 1(c) by $|r_{\text{eff}}|$ produces curves with comparable magnitude: the factor $\sinh 2\eta$ introduces a $|r_{\text{eff}}|^{-1}$ suppression. The

suppression in η , which represents transitions to deeply-bound two-body states, is also responsible for the more pronounced minima in Fig. 1(a) as $|r_{\text{eff}}|$ increases for those calculations with multiple two-body bound states. The observation of interference minima in K_3 is thus more favorable near a narrow Feshbach resonance.

Equations (8) and (9) further reveal the importance of the short-range three-body physics through their dependence on A in both η and Φ . This physics is absent from the zero-range treatments [14, 23], so the agreement in Fig. 1 between our numerical results and the zero-range potential predictions for the position of the first Efimov feature is rather fortuitous. We see from the arguments of \sin^2 in our analytical expressions that A -independent Efimov feature positions — as predicted in [14, 23] — are found only in the limit $\text{Re}A/|r_{\text{eff}}| \rightarrow 0$. For the numerical examples presented in Fig. 1, $\text{Re}A$ has a value comparable to r_0 , but this will not be true in general.

To get a first sense of the effect of large $|r_{\text{eff}}|$ on fermion collisions, we have studied the process $FF' + F$. For broad resonances $|r_{\text{eff}}| \approx r_0$, the $a^{-3.33}$ suppression of the relaxation rate (4) originates from a repulsive barrier in $W_{\nu\nu}(R)$ in the range $r_0 \ll R \ll a$ [21]. When $|r_{\text{eff}}| \gg r_0$, however, $W_{\nu\nu}(R)$ is modified in the range $r_0 \ll R \ll |r_{\text{eff}}|$ by the emergence of a Coulomb-like potential just as for bosons. Therefore, the repulsive barrier in that region is weakened, leading to enhanced vibrational relaxation. Moreover, when $a \ll |r_{\text{eff}}|$, the dependence of the rate on a is altered, much like the situation for bosons shown in Fig. 1(a). All of these effects can be seen in our numerical calculations shown in Fig. 3. For $a < |r_{\text{eff}}|$, relaxation scales as $(a/|r_{\text{eff}}|)^{-1}$, a much weaker suppression than for broad resonances. For $a > |r_{\text{eff}}|$, we find $V_{\text{rel}} \propto (a/|r_{\text{eff}}|)^{-3.33}$ which recovers the expected scaling with a , but has a much larger overall magnitude due to the scaling with r_{eff} . This result is consistent with the experimental observation that $^{40}\text{K}_2$ dimers were found [29, 30] to have much shorter lifetimes near a narrow resonance than $^6\text{Li}_2$ dimers close to a broad resonance [27, 28].

To summarize, we have studied ultracold collisions of three identical bosons and of mixed-spin fermions near a narrow Feshbach resonance using the connection between r_{eff} for the two-body interaction and the width of the resonance. We solved the Schrödinger equation numerically for a wide range of parameters and showed that there is still universal behavior even for finite range two-body potentials. We were able to identify the key modifications to the three-body adiabatic hyperspherical potentials and thus derive analytical expressions for the rate constants. From these analytical expressions, we showed that short-range three-body physics is still important, even near a narrow Feshbach resonance. This result is, perhaps, unfortunate for experimentalists since the positions of the Efimov features are, in general, still dependent on short-range physics, making it difficult to locate *a priori* a min-

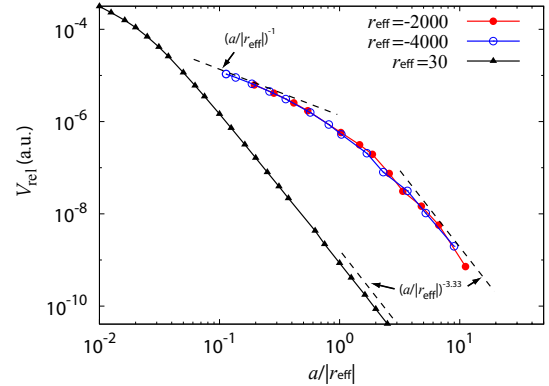


FIG. 3: Relaxation rates for mixed-spin fermions with $a > 0$ and large $|r_{\text{eff}}|$. The relaxation rate for small $|r_{\text{eff}}|$ is also plotted, showing the same scaling with a but not with $|r_{\text{eff}}|$ since it is not in the universal limit.

imum of K_3 as suggested in [14]. On the other hand, our analysis has shown that bosonic recombination and relaxation to deeply-body two-body states is suppressed near a narrow resonance which might prove beneficial experimentally. Similarly, our analysis suggests that long-lived weakly bound FF' molecules are most easily obtained near a broad resonance.

This work was supported by the National Science Foundation.

-
- [1] A. S. Jensen, K. Riisager, and D. V. Fedorov, Rev. Mod. Phys. **76**, 215 (2004).
 - [2] E. Braaten and H.-W. Hammer, Phys. Rep. **428**, 259 (2006).
 - [3] H. Feshbach, Ann. Phys. **19**, 287 (1962).
 - [4] V. Efimov, Phys. Lett. B **33**, 563-564 (1970).
 - [5] V. Efimov, Yad. Fiz. **29**, 1058 (1979).
 - [6] E. Nielsen and J. H. Macek, Phys. Rev. Lett. **83**, 1566 (1999).
 - [7] B. D. Esry, C.H. Greene, and J.P. Burke, Jr., Phys. Rev. Lett. **83**, 1751 (1999).
 - [8] T. Kraemer, *et al.*, Nature **440**, 315 (2006).
 - [9] F. Ferlaino, *et al.*, Phys. Rev. Lett. **102**, 140401 (2009).
 - [10] S. Knoop *et al.*, Nat. Phys. **5**, 227 (2009).
 - [11] T.B. Ottenstein *et al.*, Phys. Rev. Lett. **101**, 203202 (2008).
 - [12] J.H. Huckans *et al.*, Phys. Rev. Lett. **102**, 165302 (2009).
 - [13] G. Barontini *et al.*, arxiv:0901.4584 (2009).
 - [14] D. S. Petrov, Phys. Rev. Lett. **93**, 143201 (2004).
 - [15] S. Jonsell, J. Phys. B **37** S245 (2004).
 - [16] P. Massignan and H.T.C. Stoof, Phys. Rev. A **78**, 030701(R) (2008).
 - [17] G. Smirne, *et al.*, Phys. Rev. A **75**, 020702(R) (2007).
 - [18] J. Macek, Few-Body Sys. (2004).
 - [19] N. P. Mehta, *et al.* Phys. Rev. A **78**, 020701(R) (2008).
 - [20] D. S. Petrov, C. Salomon, and G. V. Shlyapnikov, Phys. Rev. Lett. **93**, 090404 (2004).
 - [21] J. P. D’Incao and B. D. Esry, Phys. Rev. Lett. **94**, 213201

- (2005).
- [22] M. Thøgersen, *et al.*, Phys. Rev. A (accepted).
 - [23] A. O. Gogolin, C. Mora, and R. Egger, Phys. Rev. Lett. **100**, 140404 (2008).
 - [24] D.V. Fedorov and A.S. Jensen, J. Phys. A **34**, 6003 (2001).
 - [25] L.H. Thomas, Phys. Rev. **47**, 903 (1935).
 - [26] M. Thøgersen, D.V. Fedorov, and A.S. Jensen, Phys. Rev. A **78**, 020501(R) (2008).
 - [27] S. Jochim, *et al.*, Science, **302**, 2101 (2003).
 - [28] S. Jochim, *et al.*, Phys. Rev. Lett. **91**, 240402 (2003).
 - [29] C. A. Regal, M. Greiner, D. S. Jin, Phys. Rev. Lett. **92**, 040403 (2004).
 - [30] C. A. Regal, M. Greiner, D. S. Jin, Phys. Rev. Lett. **92**, 083201 (2004).
 - [31] We have also used: $v(r) = (-D + B(r/r_0)^2)/(1 + (r/r_0)^8)$ and $v(r) = D((1 - e^{-(3r/r_0-1)})^2 - 1) + Be^{-2(3r/r_0-2)^2}$.
 - [32] J.P. D’Incao, C.H. Greene, and B.D. Esry, J. Phys. B **42**, 044016 (2009).
 - [33] H. Suno and B. D. Esry, Phys. Rev. A **78**, 062701 (2008).